http://www.press.ierek.com

ISSN (Print: 2357-0849, online: 2357-0857)

Environmental Science and Sustainable Development

DOI: 10.21625/essd.v7i1.869

A study on the strategies of Park City construction of Chengdu from the perspective of urban heat island mitigation

Lichen Wang[1], Kangkang Gu[1,2,*], Dong Dong[1,2]

[1]School of Architecture & Planning of Anhui Jianzhu University

[2]Anhui Academy of Territory Spacial planning & Ecology

**Corresponding author E-mail address:kangkanggu@163.com*

Abstract

In the process of urbanization, various urban problems have become increasingly prominent, and the heat island effect is one of them. The expansion of urban land, the increase in construction intensity and the increase in population make the urban heat island effect even worse. The construction of park cities improves the ecological environment of the city and is considered to have a positive effect on alleviating the heat island effect, but it is not clear whether it has such an effect or not. This article explores whether the construction of Park City can help to improve the urban thermal environment effectively, and also, seek solutions for how to improve the construction of park cities so that the heat island effect can be better mitigated. Landsat8 remote sensing images in 2014 and 2019 were used to estimate the fractional vegetation cover (FVC) and land surface temperature (LST) in the Third Ring Road of Chengdu. Land use data were also introduced into the study to analyze LST changes in different surfaces and FVC.The results indicate that: (1) the area of the heat island zone in the Third Ring Road of Chengdu decreased by 0.91% from 2014 to 2019, and the area of the cold island zone increased by 17.89% ; (2) the urban blue-green space is conductive to mitigating the urban heat island effect, in which the water provides the best mitigation, while impervious surface and bare land may aggravate the urban heat island effect; (3) the FVC in the area of the Third Ring Road in Chengdu is on the rise as a whole, and there is a significant negative correlation between FVC and LST ($p < 0.01$). Based on the above results, this paper shows that Park City construction is beneficial to alleviate the urban heat island effect, and more attention should be paid to blue-green space layout and quality, along with urban ventilation and FVC control. Our results provide useful input for green space planning and the construction of Park City in the future.

Keywords

Park City Construction; Heat island effect; Mitigation; Land cover; Fractional Vegetation Cover; Chengdu

1. Introduction

Urban heat island (UHI) refers to the phenomenon that temperatures in the urban area of a city is significantly higher than those in the outer suburbs. With the development of the economy and society, under the influence of climate change and other factors, the UHI gets increasingly obvious, which not only causes extreme weather such as hot weather and heavy rain but also negatively affects the growth of flora and fauna in cities. Medical studies show that high ambient temperature can easily lead to human irritability and mental disorders, and furthermore, it even increases the incidence of heart and respiratory diseases, thus resulting in an increase in mortality (Peng, 2020).

In recent years, scholars have carried out a large number of studies on the UHI, by two major research methods of on-site measurement and estimation based on satellite data (Ouyang et al, 2021; Amindin et al, 2021). Previous studies have focused on the following facets: the temporal and spatial characteristics, cause of formation, influencing factors, mitigation measures of UHI, the relationship between UHI and air pollution, and the impact of UHI on human health (Tian et al, 2021; Zhang et al, 2007; Park et al, 2017; Li et al, 2014; Wang et al, 2021; Laaidi et al, 2011). Studies have found that meteorological characteristics (e.g. wind speed, humidity, etc.) (Zong et al, 2021; Alekseeva et al, 2019), urban spatial morphology (e.g. building density, floor area ratio, night light intensity, etc.) (Sun, 2020; Liu et al, 2020), and land use (Singh et al, 2017) all have a certain degree of impact on the urban heat island intensity (UHII).

The research on strategies of thermal environment improvement focuses on urban ventilation, green space and water and ground materials, rational planning of urban layout and ventilation corridors and optimization of blue-green space pattern, strategies to improve the quantity and quality of green space and so on (Peng et al,2017; Guo et al, 2015; Yang et al, 2021). Among them, green spaces are considered to be able to alleviate the UHII directly and effectively, whose effect is influenced by size, shape and layout (Jonghoon et al,2017; Li et al,2014). Previous studies have shown that the cooling degree and range of green space are positively correlated with the area and negatively correlated with the shape index (Yuan et al, 2017). In further studies, scholars used models (such as CFD model) to quantitatively evaluate the impact of urban spatial morphology, land use, and other factors on urban thermal environment and proposed corresponding planning strategies to provide guidance for urban construction (Yuan et al, 2020; Iizuka et al, 2020).

In 2018, during a visit to Tianfu New Area of Chengdu, General Secretary Xi Jinping proposed the concept of "Park City" for the first time. The proposal of "Park City" not only reflects the development concept of "Ecological Civilization" and "Human-centered", but also reflects the consideration of the development mode and the pathway of urbanization. In recent years, Chengdu has made persistent efforts to advance the construction of Park City. Related theoretical studies mainly focus on the construction strategies, paths and ecological value of Park Cities, including constructing ecological network systems, promoting park layout optimization, shaping city style, innovating park management mode and so on (Lin et al, 2020). However, the current studies have not yet covered the impact of Park City construction on the urban thermal environment. Although Park City construction helps to increase the urban blue-green space and improve quality, it is still not clear whether the Park City construction can effectively alleviate the UHI. Therefore, it is crucial to discuss how to carry out urban construction in a way to mitigate the increasing urban heat island effect more efficiently.

The purpose of this study is to determine the impact of Park City construction on the urban thermal environment, and discuss how to optimize Park City construction in order to alleviate the urban heat island effect in an even better fashion. Accordingly, we choose the Lantsat 8 satellite image and surface coverage data. Through the spatial statistical analysis and correlation analysis, we try to explore the influence of the Park City construction of Chengdu on alleviating the UHI, reaching the research conclusion on the basis of the parks in Chengdu city urban construction strategy, thus to provide further optimized guidance for the construction of Park City. In addition, we also put forward the urban strategies of Chengdu Park City construction based on the research conclusions, which give further guidance for the construction of Chengdu Park City.

2. Materials and Methods

2.1. Study area

Located in the western part of Sichuan Basin, the topography of Chengdu blocks the air flow inside the city, which brings about a significant heat island effect in Chengdu, under a subtropical monsoon humid climate. The terrain is high in the northwest and low in the southeast, and the west is dominated by deep hills and mountains, while the east is plain. The annual average temperature is about 16℃, and the UHI effect is significant. The annual frost-free period is 278 days, and the average annual precipitation is 900 ~ 1,300 mm, with low wind velocity and few sunny days. Covering a total area of 14,335 km^2, Chengdu registered an urban built-up area of 949.6km^2 in 2019, that is to say, its urbanization rate reached up to 74.41%. In recent years, Chengdu has vigorously promoted the construction of

Park City, and achieved certain results, including the newly added green space of 19 million square meters, the forest coverage of 39.9%, the green coverage of built-up area of 43.5%, and the per capita green area of parks of 14.9 m^2.

Restricted by the cloudage of study data, the study area was delineated as the inner area within the Third Ring Road in Chengdu. ArcGIS software was used to obtain the scope of the study area, that is, 19,285.29hm^2 as the total area.

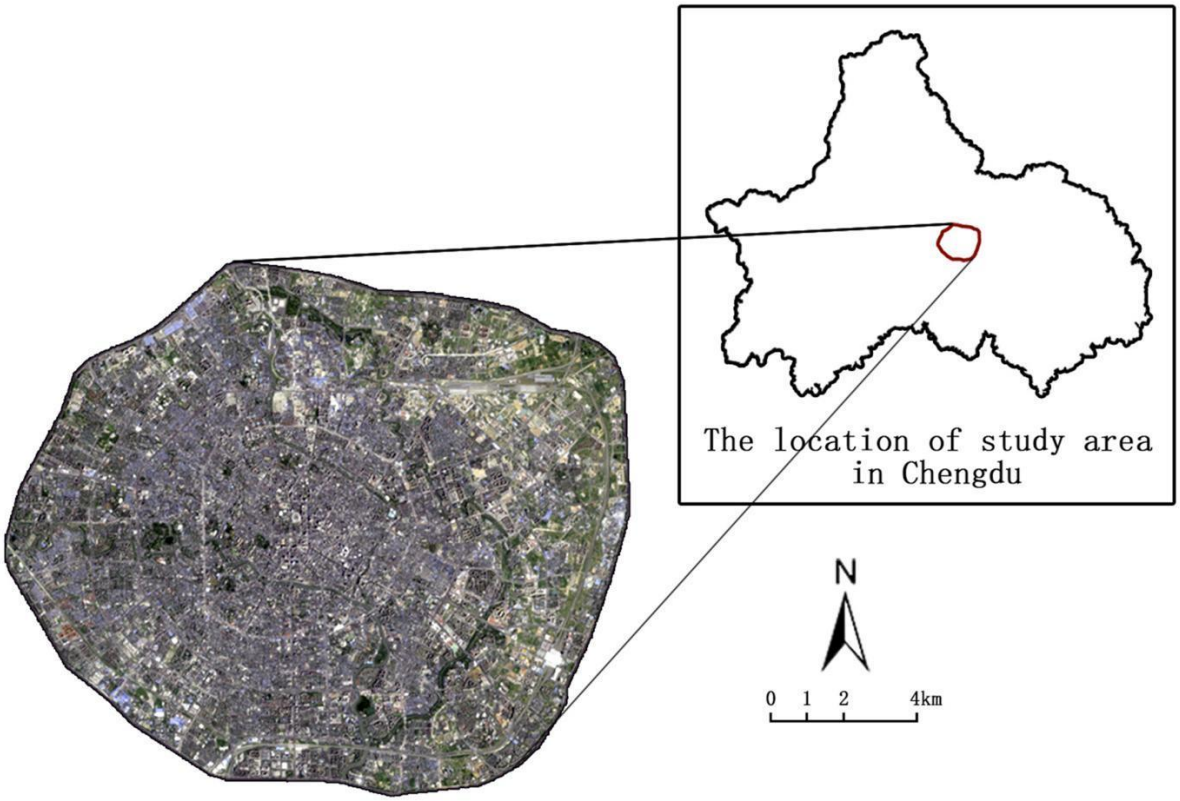

Figure 1. Satellite image of the study area

2.2. Source of data

The satellite data used in this study come from the Geospatial Data Cloud Platform of Computer Network Information Center of the Chinese Academy of Sciences (http://www.gscloud.cn). In the study, we selected Landsat8 satellite image data from August when the flora grows well. In view of the outbreak of COVID-19 in December 2019, satellite data from August 13, 2014 and August 11, 2019 were further selected for the study. The image quality was good with no cloud over the study area, which meets the research needs. Although the surface temperature retrieved by satellite remote sensing is only the surface temperature at the time of satellite transit in one day, however, the thermal field distribution characteristics of the surface of the study area are constant, so it can be used to study the distribution of the ground thermal field, and it can also cover the entire study area. The land cover data came from the Earth Big Data Science and Engineering Data Sharing Service System (http://data.casearth.cn/). The classified land cover data of 2015 and 2020 (with a spatial resolution of 30 meters) were selected to calculate the land cover of Chengdu in 2014 and 2019 respectively.

Table 1. Satellite data information

Imaging time	Satellite	Spatial resolution (m)	Cloudage	Sensor
August 13, 2014	Landsat8	30	3.74%	OLI_TIRS
August 11, 2019	Landsat8	30	0.89%	OLI_TIRS

2.3. Data pre-processing

Remote sensing has become an important way to observe UHI. Remote sensing images can cover the whole study area, and the distribution characteristics of urban heat field are stable. Therefore, remote sensing images can be used to study the spatial distribution of UHI in the study area.

Factors such as terrain, earth rotation, atmospheric refraction and others may have various influences on remote sensing imaging. In order to reflect LST as accurately as possible, ENVI5.3 software was used to conduct atmospheric correction and geometric correction on the thermal infrared image. Finally, the satellite imagery and land cover classification data were collected by using the vector layer within Chengdu's Third Ring Road.

Surface temperature inversion methods mainly include atmospheric correction method, single window algorithm, single channel method and so on. In this study, atmospheric correction method was used to process Landsat8 data and the LST was obtained by inversion. The main principle of atmospheric correction method is to evaluate the influence of atmospheric effect on surface thermal radiation based on atmospheric data, by removing the value of this part from the total thermal radiation to obtain the surface thermal radiation intensity and convert it into the corresponding LST (Wu et al, 2016), which is used to characterize the changes of UHII.

However, due to the different weather conditions at different imaging times, it is difficult to study the changes in the UHII from the inversion of the LST directly. Normalized mean-standard deviation method (Zhou, 2019) is adopted to classify UHII, that is, firstly standardize the LST, and then use the mean-standard deviation method to divide the study area into five zones: intense heat island zone (IHI), mild heat island zone (MHI), no significant zone(NS), mild cold island zone(MCI) and intense cold island zone (ICI).

2.4. Analytical techniques

2.4.1. Land cover and UHII

The research superimposed the land cover data and LST data in the inner area within the Third Ring Road of Chengdu in 2014 and 2019, calculated the average LST of various types of land cover respectively, and made statistics on the types of land cover in different UHII grading zones. Finally, we got the land cover data in each zone. The purpose of this analysis is to determine the influence of various land cover types on LST.

Considering that the LST obtained by satellite data inversion may be affected by weather conditions, in order to intuitively analyze the different effects of different urban land cover types on UHII, we choose to measure the impact of land use change on LST based on the average LST change value of different areas. Therefore, this paper divides the study into different zones according to the different land cover types in the inner area within the Third Ring Road of Chengdu in 2014. Arcgis software was used to calculate the average LST of each zone in 2014 and 2019 and obtain the LST change, which was used as the basis to measure the change of UHII.

After that, we counted the land cover types of each zone in 2019 and further divided them into smaller zones. Then, we calculated the average LST of each smaller zone in 2014 and 2019, subtracted the LST change obtained here from the average LST change mentioned above, and finally, conducted quantitative analysis of the changes of UHII in different land cover zones (a positive result means a rise in LST, which means an increase in UHII. A negative result means a drop in LST, which means a decrease in UHII).

2.4.2. Calculation of Fractional Vegetation Cover (FVC)

In the study, we used the pre-processed data to calculate the Normalized Difference Vegetation Index (NDVI), and then converted the specific values outside the interval into the background value (0) to calculate the FVC:

$$FVC = (NDVI - NDVI_{soil})/(NDVI_{veg} - NDVI_{soil}) \quad (1)$$

In the formula, $NDVI_{veg}$ is the NDVI of pure vegetation-covered pixel, and $NDVI_{soil}$ is the NDVI of bare soil-covered pixel.

In this study, FVC is divided into five grades, and the classification criteria are as follows: [0, 0.2] is low FVC, (0.2, 0.4] is medium-low FVC, (0.4, 0.6] is moderate FVC, (0.6, 0.8] is medium-high FVC and (0.8, 1]is high FVC (Peng et al, 2017). The FVC of different UHII zones was analyzed by Arcgis software.

3. Results

3.1. Spatial distribution characteristics of UHII

The LST retrieved from Landsat8 images can be obtained through data processing by Arcgis. The average LST of the study area on August 13, 2014 was 35.89℃, and the temperature distribution ranged 26.39℃ to 47.86℃. On August 11, 2019, the average LST was 40.21℃, and the temperature distribution ranged 29.80℃ to 49.81℃. In this study, we divided the study area into five zones (Fig. 2). The area and proportion of each zone are shown in Table 2.

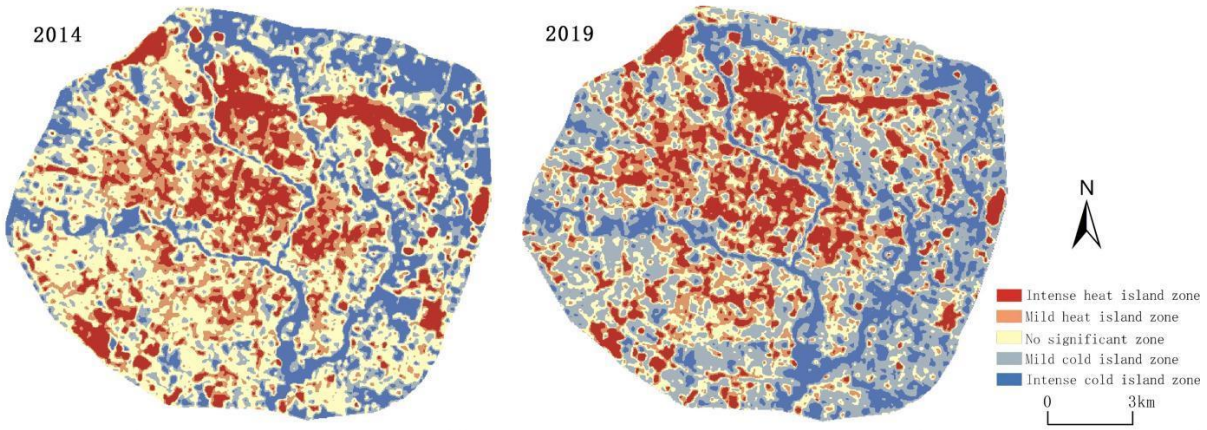

Figure 2. Classification of UHII within the Third Ring Road of Chengdu in 2014 and 2019

Table 2. Classification of SUHII

SUHII	Range	2014		2019		Value change[1]
		Area (hm^2)	Proportion (%)	Area (hm^2)	Proportion (%)	
IHI	Ts≥(a+Sd)	2,929.23	15.19	2,874.33	14.90	-
MHI	(a+0.5*Sd)≤Ts<(a+Sd)	3,202.11	16.60	3,081.78	15.98	-
NS	(a−0.5*Sd)≤Ts<(a+0.5*Sd)	7,138.62	37.02	3,864.42	20.04	-
MCI	(a−Sd)≤Ts<(a−0.5*Sd)	2,815.74	14.60	6,578.73	34.11	+
ICI	Ts<(a−Sd)	3,199.59	16.5	2,886.03	14.96	-

[1] *"+" represents an increase in area from 2014 to 2019; "-" represents a decrease in area from 2014 to 2019.*

Based on the above analysis, it can be concluded that: in 2014, the area of NS zone within the Third Ring Road of Chengdu is relatively large, reaching 7,138.62hm^2, accounting for 37.02% of the total area. The area of UHI is 6,131.34hm^2, accounting for 31.79% of the study area, mainly distributed in the urban center and the southwest region, which is the area with relatively concentrated construction land with low afforestation degree. In 2019, the area of MCI zone is relatively large, reaching 6,578.73hm^2, accounting for 34.11% of the study area and increasing by 3,762.99hm^2 compared with 2014. The area of UHI is 5,956.11hm^2, accounting for 30.88% of the study area, mainly concentrated in the urban center, which has decreased compared with the area in 2014.

3.2. The effect of land cover on UHII

3.2.1. Land cover in the study area

According to the land cover data, there were 8 land cover types in the study area in 2014, namely cropland, forest, grassland, shrubland, wetland, water, impervious surface and bare land. The area occupied by different land cover types in order of arrangement was as follows: impervious surface > cropland > grassland > forest > water > bareland > wetland > shrubland. In 2019, there were 6 types of land cover in the study area, including cropland, forest, grassland, water, impervious surface and bare land. The area occupied by different land cover types in order of arrangement was as follows: impervious surface > cropland > water > grassland > forest > bareland. The specific composition is shown in Table 3. As can be seen from the statistical data, in the process of Park City construction, the impervious surface within the Third Ring Road of Chengdu increased by 923.63hm^2, accounting for 4.80% of the study area, while the area of blue-green space decreased by 900.28hm^2, accounting for 4.68% of the study area.

Table 3. Statistics of land cover types in the study area

Land cover	2014		2019		Value change1
	Area（hm2）	Proportion（%）	Area（hm2）	Proportion（%）	
Cropland	1,629.37	8.46	1,026.24	5.33	-
Forest	72.03	0.37	1.61	0.01	-
Glassland	306.16	1.59	10.21	0.05	-
Shrubland	0.86	0.00	0.00	0.00	-
Wetland	3.58	0.02	0.00	0.00	-
Water	70.60	0.37	144.26	0.75	+
Impervious surface	17,143.23	89.06	18,066.86	93.86	+
Bareland	23.40	0.12	0.05	0.00	-
Total	19,249.23	100	19,249.23	100	-

[1] *"+" represents an increase in area from 2014 to 2019; "-" represents a decrease in area from 2014 to 2019.*

3.2.2. UHII in different land cover areas

In this paper, land cover data and LST data are superimposed, and the temperature of different land cover types is statistically analyzed by spatial analysis in Arcgis software. The obtained results are shown in Fig. 3. By comparison, the average LST of various land cover types in the study area in 2014 in order of arrangement was as follows: impervious surface > bare land > grassland > cropland > shrubland > forest > water > wetland, and the average LST in 2019 was as follows: bareland > impervious surface > grassland > water > forest > cropland.

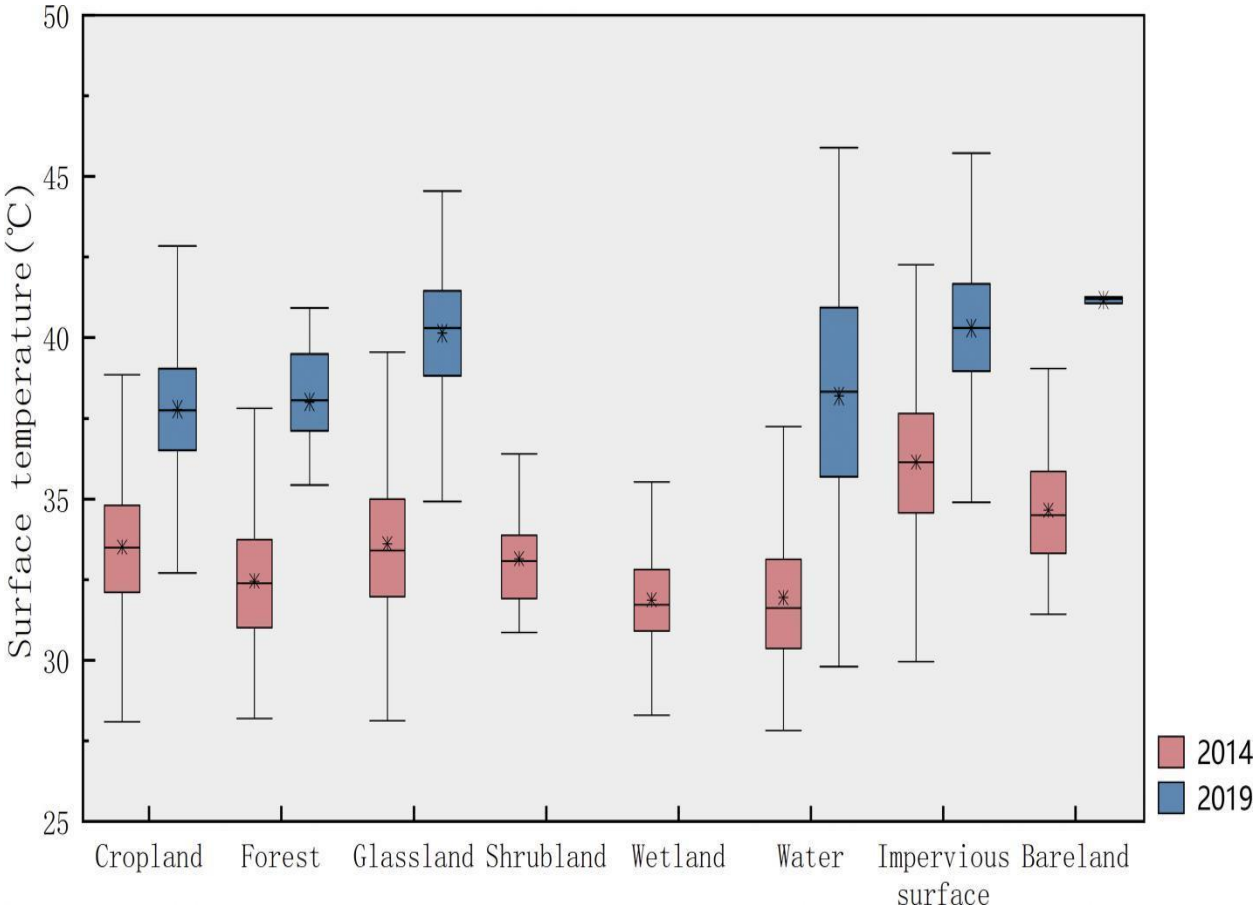

Figure 3. LST in different land cover areas

In order to analyze the relationship between UHII and land cover intuitively, statistics are made on the classification of UHII in different land cover areas, and the proportion of the obtained area is calculated to draw the classification scale diagrams of UHII of different land cover types (Fig. 4 and Fig. 5).

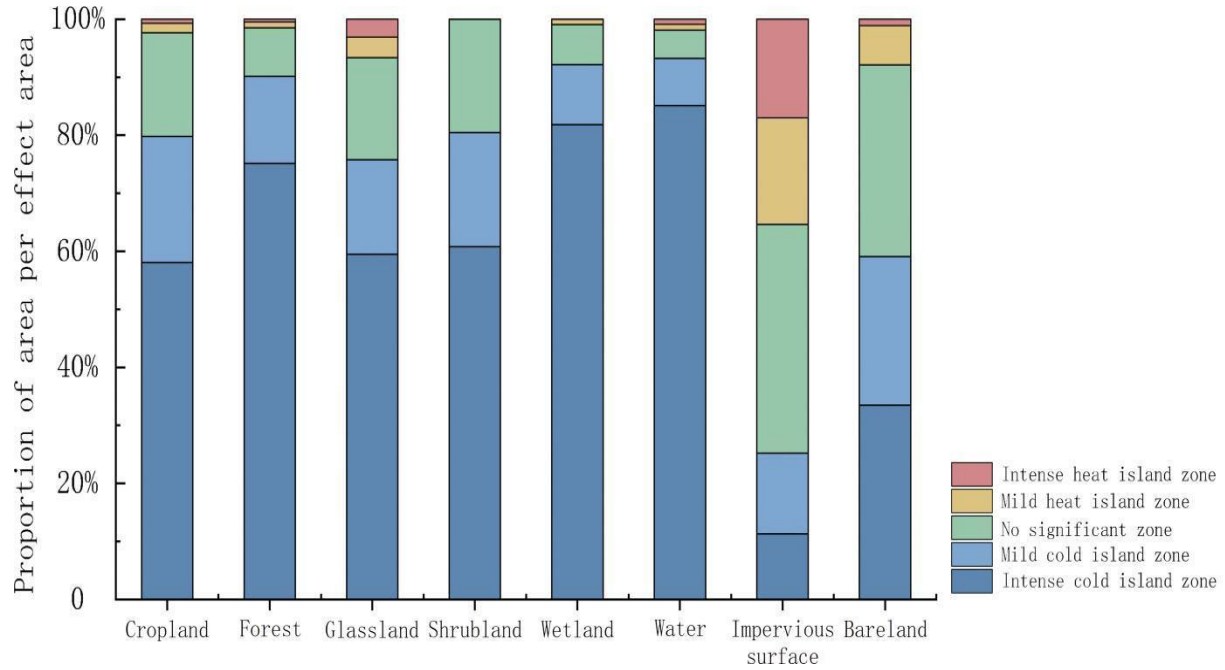

Figure 4. Scale diagram of UHII for different land cover types in 2014

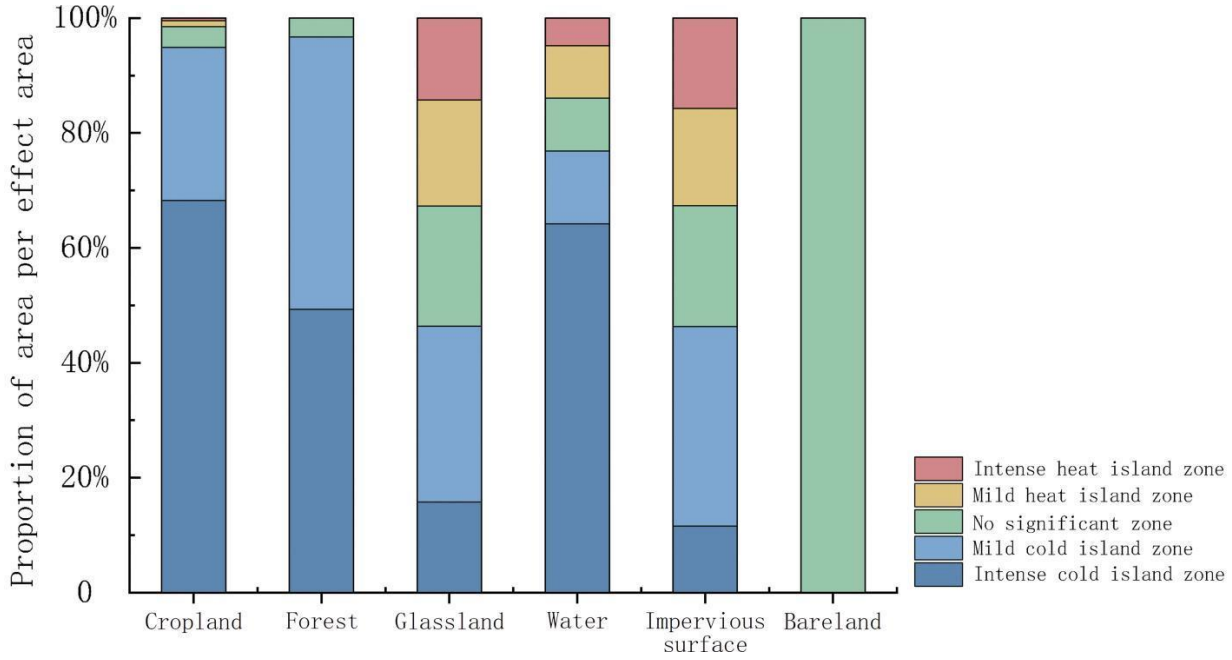

Figure 5. Scale diagram of UHII for different land cover types in 2019

From the analysis above, we found that the obvious urban cold island effect shows up in water, forest, wetland and cropland, and the LST is significantly lower than other land cover types. The LST of impervious surface and bare land in the study area was the highest, and the areas with NS zone and UHI zone accounted for a large proportion in these areas. The LST change of impervious surface, water and cropland varies more than 14℃, while the change of LST of wetland, shrub land and forest land is smaller.

3.2.3. Changes of UHII in different land cover areas

In this paper, the land use of the study area is divided into 8 zones according to the land cover situation within the Third Ring Road of Chengdu in 2014. We made statistics on the area and annual average LST of each zone and calculated the average LST change. The results are shown in Table 4. Then, we further divided each zone according to the land cover in 2019, calculated the change of LST, and compared it with the change of average LST to judge how the UHII is changing (Fig 6).

Table 4. Average LST and its variation in different land cover areas

Land cover (2014)	Area（hm2）	Average LST（℃）		Changes of LST（℃）
		2014	2019	
Cropland	1,629.37	33.17	38.16	4.99
Forest	72.03	32.23	37.09	4.86
Glassland	306.16	33.28	38.90	5.62
Shrubland	0.86	33.26	38.45	5.19
Wetland	3.58	31.92	36.92	5.00
Water	70.60	31.51	35.92	4.41
Impervious surface	17,143.23	36.24	40.46	4.22
Bareland	23.40	34.45	40.36	5.91

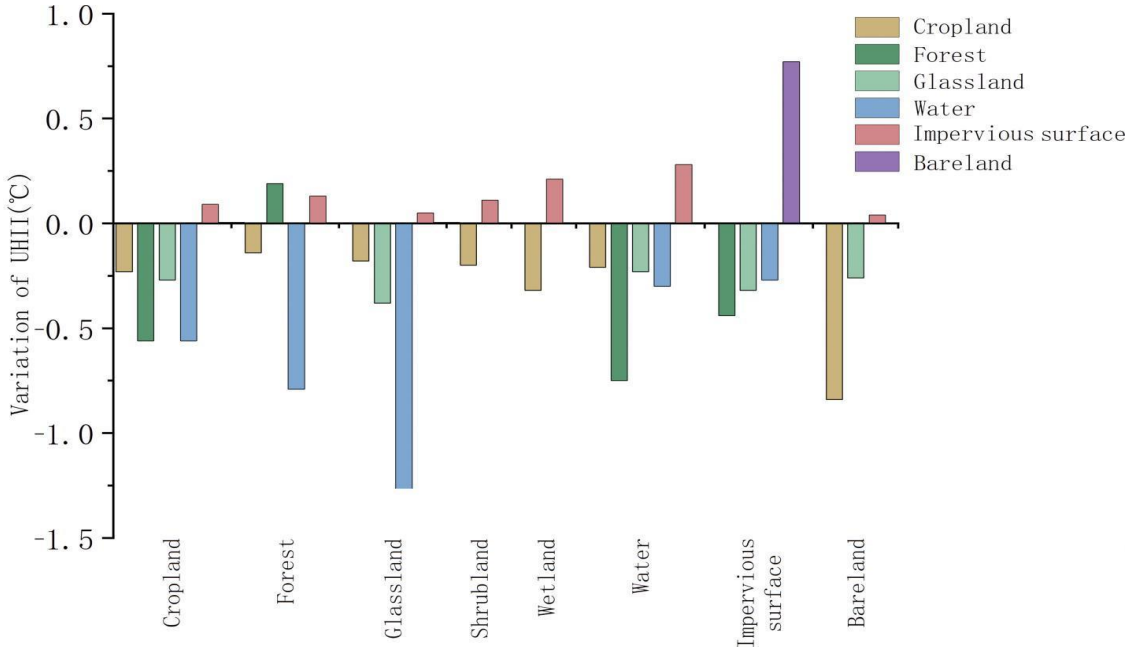

Figure 6. Variation of UHII in different land cover zones from 2014 to 2019

The above analysis shows that the UHII decreases when the land cover type is changed to cropland, grassland and water, and the UHII decreases the most when the land cover type is changed to water. The UHII increases when the land cover type is changed to impervious surface or bareland. The results of quantitative analysis indicate that blue-green space such as cropland, grassland and water is beneficial to reduce UHII, while impervious surface and bareland have negative effect on reducing UHII.

3.3. Relationships between FVC and UHII

3.3.1. Spatial distribution of FVC in the study area

Spatial distribution of FVC within the Third Ring Road of Chengdu in 2014 and 2019 is shown in Fig. 7. According to the spatial statistical analysis of Arcgis, the area of moderate FVC in the study area was the largest in 2014, up to 9,735.66hm^2, accounting for 50.48% of the study area. The area of high FVC and medium high FVC is smaller, respectively accounting for 1.97% and 13.17% of the study area. The area of low FVC is the smallest, accounting for 0.47% of the study area.

Compared with the FVC in 2014, the area of low, medium low and moderate FVC zones in 2019 in the study area decreases to varying degrees, while the area of medium high and high zones increases. The area of medium high FVC increases the most, reaching 1,027.62hm^2 (Table 5).

Table 5. Grade distribution of FVC within the Third Ring Road of Chengdu in 2014 and 2019

Zone	2014		2019	
	Area （hm2）	Proportion （%）	Area （hm2）	Proportion （%）
Low FVC zone	90.99	0.47	85.41	0.44
Medium low FVC zone	6,538.05	33.90	5,582.25	28.95
Moderate FVC zone	9,735.66	50.48	9,637.56	49.97
Medium high FVC zone	2,540.16	13.17	3,567.78	18.50
High FVC zone	380.43	1.97	412.29	2.14

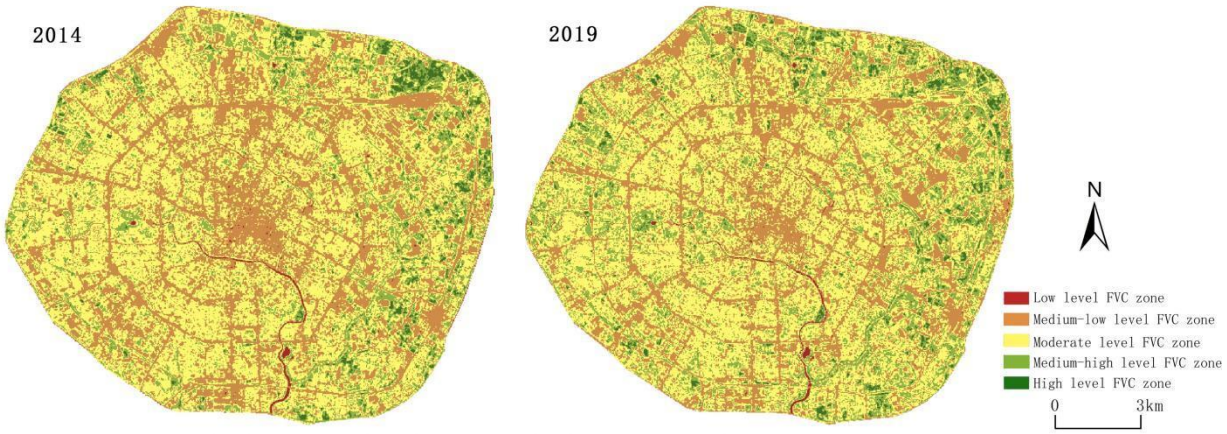

Figure 7. Spatial distribution of FVC grades within the Third Ring Road of Chengdu in 2014 and 2019

As a whole picture, the vegetation in the area within Third Ring Road of Chengdu was in good condition. After promoting the construction of the Park City, FVC has been significantly improved, and the layout of green space is more reasonable, indicating that the construction of the Park City plays an important role in promoting the realization of urban environmentally friendly and the improvement of human settlement quality.

From the perspective of spatial distribution, the area of the medium low FVC zone within the Third Ring Road of Chengdu decreased significantly from 2014 to 2019, especially in the urban center. The area of medium and high FVC expanded, spatially to the center of the city or to the west.

The area of the western part and the NS zone around the water system decreased greatly, and most of them turned into the MCI zone. Compared with the analysis of the FVC changes above, it can be found that the FVC in this area increased significantly. In general, with the construction of Park City such as urban afforestation, the area of heat island zone decreased while the area of cold island zone increased, indicating that the Park City construction has a significant positive effect on the reduction of UHII in the study area.

Table 6. Statistics of FVC in different heat island zone (hm^2)

Zone	2014				
	Low FV	Medium low	Moderate	Medium high	High
IHI	11.97	1,008.54	1,487.43	377.01	44.28
MHI	16.56	1,107.81	1,634.67	391.77	51.30
NS	33.66	2,420.64	3,576.33	952.74	155.25
MCI	12.96	930.33	1,431.27	380.34	60.84
ICI	15.84	1,070.73	1,605.96	438.30	68.76
Zone	2019				
	Low	Medium low	Moderate	Medium high	High
IHI	29.88	821.07	1,439.91	527.67	55.80
MHI	10.71	898.83	1,577.52	540.00	54.72
NS	14.40	1,128.15	1,935.54	702.63	83.70
MCI	21.78	1,884.96	3,261.15	1,259.55	151.29
ICI	8.64	849.24	1,423.44	537.93	66.78

3.3.2. Effect of FVC change on heat island effect

By importing the FVC data in 2014 and 2019, and the LST data obtained by inversion into SPSS software for correlation analysis, we find that FVC and LST showed a significant negative correlation ($P < 0.01$), indicating that the higher the FVC, the lower the LST is.

Table 7 Correlation analysis between FVC and LST

			Surface temperature	
			2014	2019
Spearman Rho	FVC	Correlation	-0.420**	-0.454**
		Number of significant (double-tailed)	0.000	0.000
		Cases	214,704	214,704

*** Significant at 99 % (P < 0.01).*

In this study, SPSS is used to fit and analyze the data, coming into a regression equation of the relationship between FVC and LST, and the Origin software is used to plot. Arcgis software is used to calculate the average LST in areas with different FVC, and the results are shown in Fig. 8 and Fig. 9.

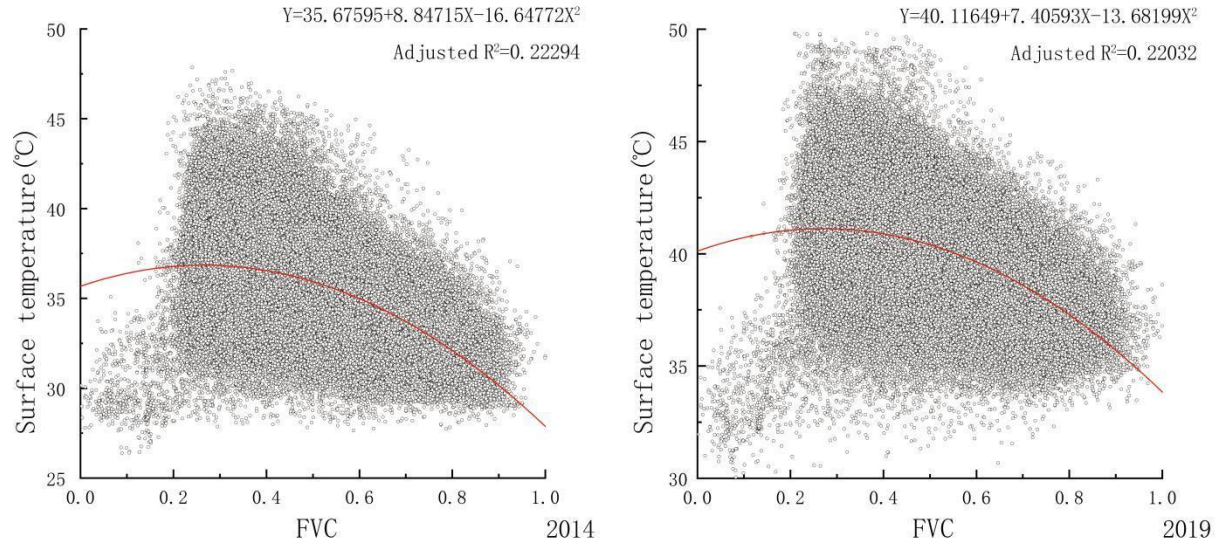

Figure 8. Fitting analysis of FVC and LST

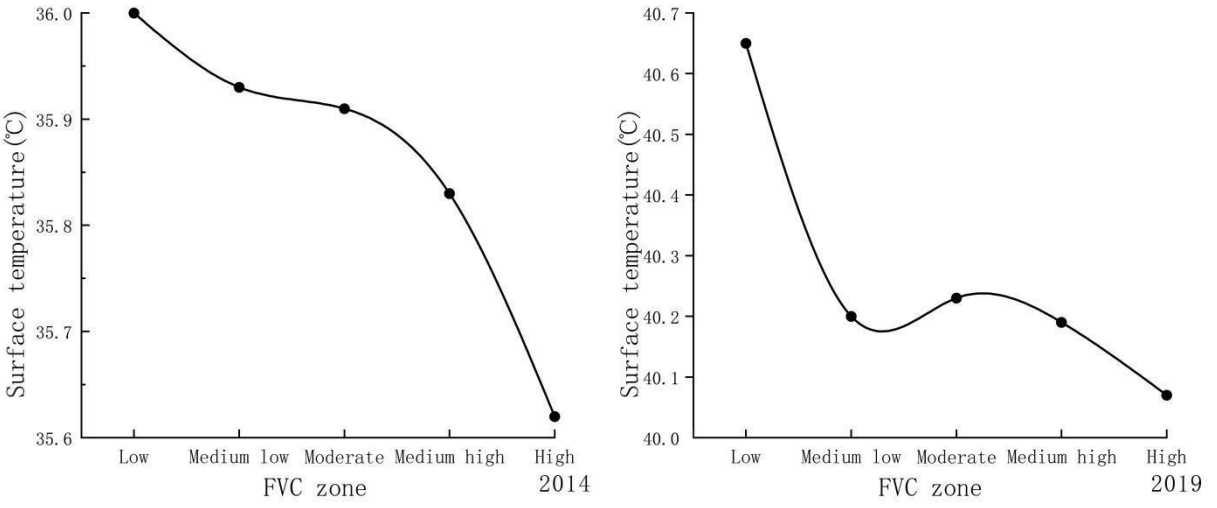

Figure 9. Average LST in different FVC zones

In the fitting equation, Y is LST (℃), X is FVC (range [0,1]). The significance of the equation $P < 0.01$.

According to the fitting analysis, compared with the low FVC and the medium low FVC zones, the LST in the moderate FVC and high FVC zones is lower. It can be seen from the statistics of average LST in different FVC zones that the LST difference between low FVC and medium low FVC, medium high FVC and high FVC zone is large, while the temperature change range among medium low FVC, moderate FVC and high FVC zone is small. The maximum average LST difference among zones with different FVC was 0.38℃ in 2014, and 0.58℃ in 2019.

The above analysis shows that, on the whole, the increase of FVC is beneficial to the reduction of UHII, although the actual cooling effect may be affected by other factors.

4. Discussion

Existing studies have shown that blue-green space is conducive to the mitigation of the heat island effect. The Park City construction aims to build an ecological civilization and create a good living environment, which is considered to have a positive effect on the improvement of urban thermal environment. In the study, we found that the heat island in Chengdu is mostly concentrated in the areas with concentrated construction land and low afforestation rate, especially in the downtown area of the city. After the construction of the Park City, the area of the heat island decreased and the area of MCI increased. Cropland, grassland, and water are beneficial to the mitigation of the heat island effect, while impervious surface and bare land may have the adverse effect. There was a noticeably negative correlation between FVC and LST.

According to the analysis on the impact of land cover and FVC on the UHII, we propose the following strategies for Park City construction of Chengdu:

- Increase the cooling effect of blue-green space
- Renovate bareland
- Control the expansion of impervious surface

This study shows that the existence of blue-green space reduces LST, while the existence of impervious surface and bareland renders it higher. UHII increases when converted to impervious surface and bareland, while UHII decreases when converted to farmland, grassland and water. Therefore, in the process of construction, attention should be paid to the protection of the ecological environment and to increase the area of urban blue-green space. Furthermore, the expansion of impervious surface and the increase of construction intensity shall be controlled, and bare land shall be eliminated and rationally utilized.

However, in the process of urban development and construction, the expansion of impervious surface is inevitable, which will inevitably compress the area of urban blue-green space. Existing studies have shown that the layout of urban green space has a notable impact on the urban meteorological environment. The cooling effect of green space on the surrounding environment is limited to a certain spatial range, yet the overall cooling effect of the decentralized green space on the surrounding environment is better than that of the centralized large green space (Luan et al, 2014; Miao et al, 2013). It can be perceived that in the process of alleviating the urban heat island effect, it is also necessary to improve the quality of the blue-green space and adjust the spatial layout appropriately in addition to ensuring the urban blue-green space. During the construction, attention should be paid to increasing the amount of green space, making full use of the existing blue-green space, and optimizing the urban blue-green space network to enhance its cooling effect.

In the downtown area of the city, the impervious surface is large but the land resources are limited, so it is not suitable to increase the large scale of urban green space. In the constructions, limited space can be used to increase the thermal comfort of a small area by appropriately adding spot-like green space or small bodies of water, which is conducive to breaking the heat island effect area and eliminating the scale effect and superposition effect of the heat island. At the same time, it can also convert the existing bare land into green space to improve the environmental quality.

- Integrate construction with urban ventilation corridor planning

Increasing air motion is one of the crucial ways to mitigate the UHII. In this study, we found that the LST of the medium low FVC zone in 2019 was slightly lower than that of the moderate FVC zone, which may be related to the presence of plants that hindered the flow of wind, resulting in agglomeration and increase of temperature. In the study of the impact of urban structure on the urban thermal environment, we can see that UHII is directly proportional to the urban building density, that is, the greater the density of urban building, the lower the air circulation efficiency, resulting in the severer heat island effect (Peng et al, 2017). In the process of Park City construction, the protection of wind sources should be strengthened and attention should be paid to creating open spaces to introduce cold air from the periphery of the city into the city. At the same time, the temperature difference between the cold and hot islands in the city should be fully utilized, and the spatial layout should be reasonably arranged to form local air circulation in the city and accelerate air motion.

- Reasonable control of FVC

Although both vegetation coverage and surface temperature showed a noticeably negative correlation, for alleviating the heat island effect, higher vegetation coverage is not always better. The quantitative analysis also reveals that the presence of forest may increase LST. Excessively high FVC will hinder air flow, cause heat accumulation and increase regional temperature, which is also one of the causes for the high temperature in Chengdu in summer. Existing studies have shown that, for different floras, the range of the effect of FVC on temperature is different (Li et al, 2021). In the process of Park City construction, plant species should be reasonably selected according to the needs, and FVC should be classified and controlled, to give full play to the cooling effect of different plants and alleviate the UHII.

The results indicated that water have a good cooling effect, and its cooling effect may be even superior to that of green space. In actual construction, water can be added to the existing green space to make full use of its mitigation effect on the heat island effect, and to reduce the accumulation of vegetation in the green space, so as to accelerate the air flow in the urban green spaces.

5. Conclusions

This study contributes to the understanding of the contribution of Park City construction to the enhancement of the urban environment, and also provides a new perspective for further optimizing Park City construction. In this paper, we used Landsat8 data and land use data to clarify the impact of Park City construction on the urban heat island effect, and found out the direction for the further improvement of urban thermal environment. The results show that there is no doubt about the Park City construction serving as the aid to the mitigation of the heat island effect, even though its effect is affected by land use and FVC. The existence of blue-green spaces is beneficial, while the impervious surface and bareland have the adverse effect; an increase in FVC is helpful in general, but in some cases, may not be. According to the results, we propose optimization strategies, including optimizing urban space layout, integrating construction with urban ventilation corridor planning and controlling FVC reasonably.

This study is expected to provide guidance for further construction given that urban heat island effect may be exacerbated later. The conclusions and the proposed strategies are useful for optimizing Park City construction and improving the quality of urban thermal environment.

References

Alekseeva, L.I., Gorlach, I.A., Kislov, A.V. (2019). Vertical structure and seasonal features of the heat island and humidity distribution over Moscow derived from satellite data[J]. Russian Meteorology and Hydrology, **44**(8): 571-578. https://doi.org/10.3103/S1068373919080090

Amindin, A., Pouyan, S., Pourghasemi, H.R., Yousefi, S., Tiefenbacher, J.P. (2021). Spatial and temporal analysis of urban heat island using Landsat satellite images[J]. Environmental Science and Pollution Research, **28**(30): 41439-41450. https://doi.org/10.1007/S11356-021-13693-0

Guo, G.H., Wu, Z.F., Xiao, R.B., Chen, Y.B., Liu, X.N., Zhang, X.S. (2015). Impacts of urban biophysical composition on land surface temperature in urban heat island clusters[J]. Landscape and Urban Planning, **135**: 1-10. https://doi.org/10.1016/j.landurbplan.2014.11.007

Iizuka, S., Xuan, Y.L., Takatori, C., Nakaura, H., Hashizume, A. (2020). Environmental impact assessment of introducing compact city models by downscaling simulations[J]. Sustainable Cities and Society, **63**: 102424.4. https://doi.org/10.1016/j.scs.2020.102424

Laaidi, K., Zeghnoun, A., Dousset, B., Bretin, P., Vandentorren, S., Giraudet, E., Gourmelon, F., Pascal, M. (2011). Health Impact of Heat Waves in Urban Heat Islands: How to Estimate the Exposure of the Population?[J]. Epidemiology, **22**(1s): S22-22. https://doi.org/10.1097/01.ede.0000391725.38993.c9

Li, S.L., Feng, L., Cao, S., Jia, B.W., Wang, Q.Y., Ma, X.Y. (2021). Effects of vegetation coverage of phytocoenosium on green space temperature in Beijing [J]. Journal of Beijing University of Agriculture, **36**(03): 88-94. https://doi.org/10.13473/j.cnki.issn.1002-3186.2021.0316

Li, X.Z., Li, H.Y., Zhang, Q.T., Qiu, G.Y. (2014). Study on reducing effect of different urban landscapes on urban temperature[J]. Ecology and Environmental Sciences, **23**(01): 106-112. https://doi.org/10.16258/j.cnki.1674-5906.2014.01.009

Lin, K.X., Ni, J.J., Zhou, M. (2020). Origin of thought, cognition of value, and planning path of Park City[J]. Planners, **36**(15): 19-24.

Liu, J., Shen, L., Huang, Y., Deng, X. (2020). Research on the spatial differentiation of characteristics of nocturnal urban heat island intensity in Beijing based on local climate zones[J]. Geography and Geo-information Science, **36**(05): 39-45+64.

Luan, Q.Z., Ye, C.H., Liu, Y.H., Li, S.Y., Gao, Y.H. (2014). Effect of urban green land on thermal environment of surroundings based on remote sensing: A case study in Beijing, China[J]. Ecology and Environmental Sciences, **23**(02): 252-261. https://doi.org/10.16258/j.cnki.1674-5906.2014.02.004

Miao, S.G., Wang, X.Y., Jiang, W.M., Wang, Y.W., Chen, X.Y. (2013). Impact on atmospheric environment by green space layout in urban planning: A case study on green space planning of Chengdu[J]. City Planning Review, **37**(06): 41-46.

Park, J., Kim, J.H., Lee, D.K., Park, C.Y., Jeong, S.G. (2017). The influence of small green space type and structure at the street level on urban heat island mitigation[J]. Urban Forestry & Urban Greening, **21**: 203-212. https://doi.org/10.1016/j.ufug.2016.12.005

Ouyang, W., Morakinyo, T.E., Ren, C., Liu, S., Ng, E. (2021). Thermal-irradiant performance of green infrastructure typologies: Field measurement study in a subtropical climate city[J]. Science of the Total Environment, **764**: 144635. https://doi.org/10.1016/j.scitotenv.2020.144635

Peng, W.F., Zhou, J.M., Xu, X.L., Luo, H.L. (2017). Dynamic monitoring of fractional vegetation cover in Chengdu Plain and its surrounding area in China[J]. Earth and Environment, **45**(02): 193-202. https://doi.org/10.14050/j.cnki.1672-9250.2017.02.011

Peng, X., Liu, X.Y., Xu, Y., Shu, J.S., Liu, M.J., Xu, D.H. (2017). Preliminary analysis of measures to alleviate the heat island effect[J]. Contemporary Horticulture, **64**(9): 112-114. https://doi.org/10.14051/j.cnki.xdyy.2017.17.064

Peng, Y.G. (2020). Heat wave characteristics, mortality and effect modification by temperature zones: a time-series study in 130 counties of China, **100**(34): 2704. https://doi.org/10.3760/cma.j.issn.0376-2491.2020.34.102

Singh, P., Kikon, N., Verma, P. (2017). Impact of land use change and urbanization on urban heat island in Lucknow city, Central India. A remote sensing based estimate[J]. Sustainable Cities and Society, **32**: 100-114. https://doi.org/10.1016/j.scs.2017.02.018

Sun, Z. (2020). Impact of urban morphology factors on thermal environment in high density urban areas: A case of Beijing within 5th Ring Road[J]. Ecology and Environmental Sciences, **29**(10): 2020-2027. https://doi.org/10.16258/j.cnki.1674-5906.2020.10.012

Tian, P., Li, J.L., Cao, L.D., Pu, R.L., Wang, Z.Y., Zhang, H.T., Chen, H.L., Gong, H.B. (2021). Assessing spatiotemporal characteristics of urban heat islands from the perspective of an urban expansion and green infrastructure[J]. Sustainable Cities and Society, **74**: 103208. https://doi.org/10.1016/J.SCS.2021.103208

Wang, Y.Y., Guo, Z.Y., Han, J. (2021). The relationship between urban heat island and air pollutants and them with influencing factors in the Yangtze River Delta, China[J]. Ecological Indicators, **29**: 107976. https://doi.org/10.1016/J.ECOLIND.2021.107976

Yang, P., Cheng, S.Y., Gao, Q., Zhi, L.H., Zhang, Y.P., Zhou, J.B., Zhou, Y. (2021). Spatio-temporal evolution and interrelationship between underlying surface types and thermal environment in the main urban area of Shijiazhuang city[J]. Hubei Agricultural Sciences, **60**(20): 48-56. https://doi.org/10.14088/j.cnki.issn0439-8114.2021.20.009

Yuan, C., Adelia, A.S., Mei, S.J., He. W.H., Li, X.X., Norford, L. (2020). Mitigating intensity of urban heat island by better understanding on urban morphology and anthropogenic heat dispersion[J]. Building and Environment, **176**: 106876. https://doi.org/10.1016/j.buildenv.2020.106876

Yun, Z., Wu, X.L., Zang, S.Y., Wu, C.S., Li, M. (2017). Cooling effect of green patches based on TM image in Harbin downtown city[J]. Scientia Geographica Sinica, **37**(10): 1600-1608. https://doi.org/10.13249/j.cnki.sgs.2017.10.018

Zhang, K.Y., Xu, C.X., Cui, G.X., Zhang, Z.S., Wang, Z.S. (2007). Numerical simulation of urban heat island evolution and its effect on pollutant transport[J]. Journal of Meteorology and Environment, **23**(03): 10-14.

Zong, L., Liu, S.H., Yang, Y.J., Ren, G.Y., Yu, M., Zhang, Y.H., Li, Y.B. (2021). Synergistic influence of local climate zones and wind speeds on the urban heat island and heat waves in the megacity of Beijing, China[J]. Frontiers in Earth Science, **9**: 673786. https://doi.org/10.3389/FEART.2021.673786